scientific reports

Check for updates

OPEN

Knockout of protein arginine methyltransferase 1 inhibited cell growth and promoted cell migration in human bronchial epithelial cells

Wen-Jing Yang, Bing-Yan Liu & Lu Xue✉

Previous studies have demonstrated that PRMT1 was involved in the progression of multiple lung diseases. However, its specific function within the bronchial epithelium was still limited and needed further exploration. In the present study, human bronchial epithelial cell line 16HBE was chosen to elucidate the biological role of PRMT1 in lung epithelium. Cell proliferation, cell-cycle distribution, cell apoptosis, and cell motility capacity were systematically evaluated following CRISPR/Cas9-mediated knockout of PRMT1. We showed that knockout of PRMT1 in 16HBE inhibited cell proliferation, redistributed cell cycle, promoted cell apoptosis, and accelerated cell migration via a series of regulated cyclins, cyclin-dependent kinase regulators, and EMT markers. Taken together, these findings identify PRMT1 as a potential modulator of epithelial cell proliferation, survival, and motility in the human bronchial epithelium, offering new insights into its possible role in epithelial remodeling during pulmonary disorders.

Keywords PRMT1, Bronchial epithelium, Cell proliferation, Cell migration

Abbreviations

AR	Androgen receptor
Bcl-2	B-cell lymphoma-2
CDC2	Cell division cycle 2 kinase
CDK	Cyclin-dependent kinases
CDKIs	Cyclin-dependent kinase inhibitors
DMSO	Dimethyl sulfoxide
EGFR	Epidermal growth factor receptor
EMT	Epithelial-mesenchymal transition
EZH2	Enhancer of zeste homolog 2
FBS	Fetal bovine serum
H4R3me2a	Asymmetric dimethylation of histone H4 on arginine 3
OD	Optical density
PBS	Phosphate-buffered saline
PTM	Post-translational modification
PRMTs	Nine arginine methyltransferases

Arginine methylation is a common and widespread post-translational modification (PTM) that regulates numerous biological processes[1]. According to the type of arginine methylation produced, nine arginine methyltransferases (PRMTs) have been divided into three families (type I PRMT1, type II PRMT1, and type III PRMT1)[2]. Protein arginine methyltransferase 1 (PRMT1), a major member of the type I PRMT family, is responsible for 85% of cellular PRMT activity, through catalyzing monomethylation and asymmetric demethylation of arginine side chains in proteins[3].

Institute for Medical Biology and Hubei Provincial Key Laboratory for Protection and Application of Special Plants in Wuling Area of China, College of Life Sciences, South-Central Minzu University, 182 Minyuan Road, Hongshan District, Wuhan 430074, China. ✉email: sparkler830305@hotmail.com; xuelu@mail.scuec.edu.cn

Many studies have demonstrated that PRMT1 played an important role in embryogenesis and development[4–7]. Moreover, dysregulation of PRMT1 contributed to multiple physiological processes in various adult organs. In the heart, PRMT1 played a critical role in the cardiac repolarization[8], and the ablation of PRMT1 caused heart failure through CaMKII dysregulation[9]. In the liver, PRMT1 protected the liver from alcohol-induced injury by modulating oxidative stress responses[10]. In the kidney, the inhibition of PRMT1 alleviated acute kidney injury by inactivating the TGF-β1/Smad3 pathway in the cortex and IL-6/STAT3 pathway in the medulla[11]. In the gut, PRMT1 could regulate gut microbiota modulation and be a useful marker for hischsprung's disease[12,13]. Our previous study also found that conditional knockout of PRMT1 in the intestine could affect the formation and differentiation of the intestinal epithelium[14–16].

Taken together, PRMT1 was shown to play a vital role in a series of physiological processes and has potential as a therapeutic target. Based on this, several PRMT1 inhibitors have been investigated. For example, DCPT1061 is a small-molecule inhibitor of PRMT1 that has broad applications in tumor immunotherapy and in overcoming resistance to immune checkpoint inhibitors[17]. MS023 and GSK3368715, PRMT1 inhibitors, increased tumor-infiltrating lymphocytes in a cGAS-dependent manner and promoted tumor PD-L1 expression[18].

With the intensification of industrialization, urbanization, and global environmental pollution, the etiology of lung disease has become more complex, and exploring new diagnostic and treatment methods is of great significance[19,20]. In recent years, there has been increasing research on PRMT1 in lung diseases[21]. It was found that PRMT1 expression was significantly increased in lung tissue sections and isolated airway smooth muscle cells of severe asthma patients. Bronchoplasty reduced airway remodeling by blocking the expression of PRMT1 in fibroblasts[22]. Inhibition of PRMT1 eliminated the deposition of type I collagen and fibronectin, cell proliferation, and migration of airway smooth muscle cells in asthma patients[23]. PRMT1 could activate STAT1 or RUNX1, then stimulate the expression of let-7i and miR-423, which were essential for the airway remodeling of asthma[24]. PRMT1 could also regulate epithelial-to-mesenchymal (EMT) in non-small cell lung cancer via Arg-34 methylation of Twist1[25]. The above studies indicated that PRMT1 was involved in the epithelium dysfunction of pulmonary diseases. However, research on the biological role of PRMT1 in the lung epithelium remains limited and requires further investigation. 16HBE was a typical human bronchial epithelial cell line isolated from a 1-year-old male heart–lung patient and has been widely used in studies of pulmonary diseases, including airway inflammation[26], airway epithelial injury[27], and cancer[28]. In the present study, 16HBE was chosen to explore the biological function of PRMT1 in pulmonary diseases, providing potential drug targets for the treatment of respiratory-related diseases.

In the present study, we demonstrated that knockout of PRMT1 in 16HBE influences cell proliferation, cell cycle, cell apoptosis, and cell migration, which are essential processes during epithelial dysfunction, especially EMT. Taken together, we proved that PRMT1 was a novel regulator of cell physiological processes in human bronchial epithelium. Moreover, PRMT1 could also emerge as a potentially important biomarker for bronchial epithelial disease.

Materials and methods

Establishment of PRMT1 knockout cell lines

The human bronchial epithelial cell line 16HBE was purchased from Zhongqiaoxinzhou Biotech (Shanghai, China). The PRMT1 knockout 16HBE cell lines were established as previously described[29,30] with subtle revision. Briefly, a recombinant plasmid named px458-PRMT1-sgRNA2[29] (inserted sgRNA sequences: 5′-GGATGTCA TGTCCTCAGCG-3′) was transfected into 16HBE cells with Lipofectamine 3000 (Thermo Fisher Scientific, San Jose, CA, USA). Then green fluorescence-positive cells were isolated via a SH800S flow cytometer (Sony, Tokyo, Japan) according to the manufacturer's instructions. The isolated single cell was cultured in 96 plates with DMEM medium (Gibco, NY, USA) supplemented with 10% fetal bovine serum (Biological Industries, Kibbutz Beit-Haemek, Israel). The expression of PRMT1 in edited cells was detected via western blotting. Two PRMT1 knockout 16HBE cell lines (named as 16P-2 and 16P-11) were selected for further experiments. Wild-type 16HBE cell line (named as WT), which was transfected with px458, was applied as a control. Subsequent experiments were performed after the cells had been passed on for 2–3 times.

Cell proliferation analysis

The cell proliferation was analyzed through the MTT assay and colony formation assay. In the MTT assay, WT, 16P-2, and 16P-11 cells were seeded in 96-well plates at a density of 2000 cells/well, respectively. Then the adherent cells were treated with 20 μL 5 mg/mL MTT (Biofroxx, Shanghai, China). After 4 h incubation at 37 °C, the supernatant was removed and 150 μL dimethyl sulfoxide (DMSO, Macklin, Shanghai, China) was added to each well. The optical density (OD) value at 490 nm was measured with Infinite® M200 Pro (TECAN, Manedorf, Switzerland) at 0h, 24 h, 48 h, 72 h, and 98 h, respectively. The rate of cell proliferation was calculated as follows: OD value of each day/OD value on the first day. Each group (WT, 16P-2, and 16P-11) had six replicates.

In the colony formation assay, approximately 200 cells were seeded in 6-well plates and cultured for 2 weeks. The colonies were fixed with 500 μL paraformaldehyde (Biosharp, Beijing, China) for 30 min. Then the fixed colonies were stained with 400 μL Wright's Giemsa A for 2 min (Biosharp, Guangzhou, China) and 800 μL Wright's Giemsa B for 5 min, subsequently. After washing with ultra-pure water three times, the colonies in each plate were imaged and counted. The percentage of colonies was calculated as follows: clone counts/200 × 100%. Each group (WT, 16P-2, and 16P-11) had three replicates. All the data were analyzed with GraphPad Prism 7.00 (https://www.graphpad.com/, GraphPad Software, San Diego, CA, USA).

Cell cycle analysis

When the density of the cells (WT, 16P-2 and 16P-11 groups, respectively) reached approximately 85%, the cells were pelleted and fixed in 70% ethanol for 4 h at 4 °C. After fixation, 70% ethanol was removed, and the

cells were washed twice with ice-cold phosphate buffered saline (PBS, Hyclone, Walthma, MA, USA). Then the collected cells were gently resuspended in 500 µL of PI solution (Antgene, Wuhan, China) and incubated at 37 °C for 30 min. The distribution of the cell cycle was detected via a BD FACS Calibur flow cytometer (BD Biosciences, San Jose, CA, USA) according to the manufacturer's instructions. Each group (WT, 16P-2, and 16P-11) had three replicates. Finally, the data were visualized with ModFit LT 5.0 (https://vsh.com/, Verity Software House, Topsham, ME, USA), and the percentage of cell phases (G1, S, and G2/M) was analyzed with GraphPad Prism 7.00.

Cell apoptosis analysis

The cells for apoptosis analysis (WT, 16P-2, and 16P-11 groups, respectively) were cultured in 6-well plates, and the confluence reached approximately 85%. Then pelleted cells were washed twice with PBS. According to the protocol of the Annexin VFITC Apoptosis Detection Kit (Dojindo, Shanghai, China), 500 µL 1 × Annexin V Bind Buffer and 5 µL Annexin V were added into each sample, subsequently. After incubation for 5 min, 5 µL PI solution was added to the above suspension and incubated for 15 min. After the addition of 400 µL 1 × Annexin V Bind Buffer, the mixed cells were filtered with a 48 µm nylon membrane, and the cell apoptosis was assessed via a BD FACS caliber flow cytometer according to the manufacturer's instructions. Each group (WT, 16P-2, and 16P-11) had three replicates. Finally, the data was visualized with ModFit LT 5.0, and the percentage of apoptotic cells was analyzed with GraphPad Prism 7.00.

Cell motility analysis

Cell motility was analyzed through the wound healing assay and invasion assay. WT, 16P-2, and 16P-11 groups were seeded in a 12-well plate with a density of 4×10^5 cells. When cells achieved approximately 90% confluence, a wound was created by scraping the cell layer with a sterile 10 µL pipette tip. After replacing the culture medium with serum-free medium, the wounds were photographed at 0 h, 6 h, and 12 h, respectively. The healing rate was calculated as follows: (the wound width at 0 h—the wound width at 6 h/12 h) / the wound width at 0 h × 100%.

For the cell invasion assay, approximately 5×10^4 cells (WT, 16P-2, and 16P-11, respectively) were seeded in the top chambers of a 24-well transwell® plate (8.0 µm pore size; Corning Costar, Corning, NY, USA) with 200 µL DMEM without serum. 700 µL DMEM supplemented with 10% fetal bovine serum (FBS) was added to the bottom chamber. After incubation at 37 °C for 48 h, the rest cells on the top side of the filter were wiped out with a cotton swab, while those on the bottom side (those that had migrated) were fixed with 4% polyoxymethylene for 30 min, and stained with Giemsa staining solution (Biosharp, Guangzhou, China). Each group had three replicates. Five randomly selected fields per well were photographed, and the number of cells was counted with Image J 1.52a (http://imagej.nih.gov/ij, Wayne Rasband, National Institutes of Health, USA). The data was analyzed with GraphPad Prism 7.00.

Western blot analysis

The WT, 16P-2, and 16P-11 cells were lysed with protein lysis buffer (Beyotime, Shanghai, China) to extract total proteins. The protein samples (20 µg per lane) were separated with 8% ~ 15% SDS-PAGE gel (EpiZyme, Shanghai, China) according to the molecular weight of the proteins. After electrophoresis, proteins were transferred to PVDF membranes (Millipore, MA, USA) and detected with the corresponding antibodies (Cell Signaling Technology, Beverly, MA, USA). ECL reagent (Yeasen, Shanghai, China) was used to visualize the protein bands through ChemiDoc XRS + (Bio-Rad, Hercules, CA, USA), and the samples were quantitatively assessed by ImageLab software (Bio-Rad, Hercules, CA, USA). β-Actin or GAPDH was used as an internal control.

Statistical analysis

All assays were repeated at least three times. GraphPad Prism version 7.00 was used to perform statistical analyses of the experimental data. Student's unpaired t-test was applied to compare the differences between the two groups. $P < 0.05$ was considered statistically significant.

Results

Knockout of PRMT1 inhibited cell proliferation in 16HBE

To investigate the role of PRMT1 in human bronchial epithelium, the 16HBE cell line was chosen to establish the PRMT1 knockout cell line via CRISPR/Cas9 technology as our previous study[29,30]. Compared with the WT group, the expression of PRMT1 in knockout cell lines (16P-2 and 16P-11) was nearly undetectable, which indicated that PRMT1 has been successfully knocked out (Fig. 1A). Furthermore, the MTT assays showed that the rate of cell proliferation was significantly inhibited in 16P-2 and 16P-11 (Fig. 1B), which was consistent with the results of knocking out PRMT1 in 293 T cells[29]. Meanwhile, the colony formation assay confirmed that PRMT1 knockout could suppress cell growth (Fig. 1C, D). Further western blot showed that the expression level of c-Myc, which was a key regulatory factor in epithelial cell proliferation[31,32], was upregulated in 16P-2 and 16P-11 (Fig. 1E). Moreover, the phosphorylation of AKT, another key factor related to airway epithelial proliferation[33], was upregulated too (Fig. 1F). In recent years, research has found that the c-Myc gene was also closely related to cell apoptosis, with a dual effect of stimulating cell proliferation and apoptosis[34]. A possible explanation of the inhibition of cell proliferation in PRMT1 knockout 16HBE cells was that the upregulation of p-AKT activated the proapoptotic effect of c-Myc, thereby inhibiting cell proliferation.

Knockout of PRMT1 redistributed the cell cycle in 16HBE

To investigate the underlying mechanism of inhibited cell growth in the PRMT1 knockout 16HBE cell line, cell cycle analysis was conducted via flow cytometry. It was found that knockout of PRMT1 decreased the proportion

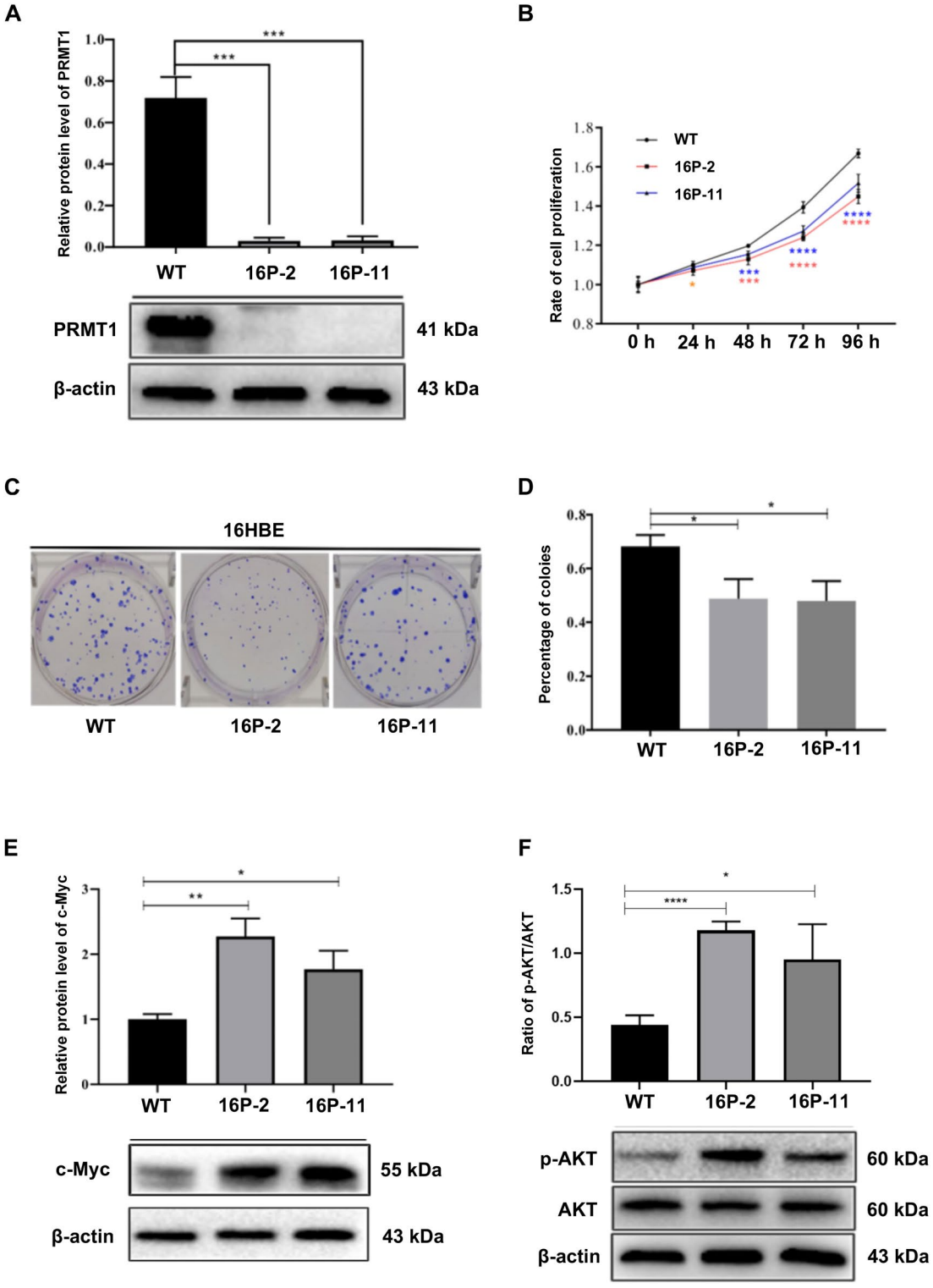

Fig. 1. Knockout of PRMTA1 inhibited cell growth in 16HBE. (**A**) Western blot results showed that PRMT1 knockout 16HBE cell lines were successfully established. Upper, bar graph; lower, representative blots. (**B**) Knockout of PRMT1 inhibited cell proliferation in 16HBE. (**C**) Knockout of PRMT1 reduced colony formation in 16HBE. (**D**) The bar graph showed the percentage of colonies in WT, 16P-2, and 16P-11, respectively. (**E**) Western blot results showed that c-Myc was upregulated in PRMT1 knockout cell lines. (**F**) PRMT1 knockout elevated AKT phosphorylation. *, $p < 0.05$; **, $p < 0.01$; ***, $p < 0.001$; ****, $p < 0.0001$.

of cells in G1 phase and G2/M phase, while the proportion of S phase cells responsible for DNA synthesis was significantly increased (Fig. 2A, B). In conclusion, knockout of PRMT1 led to S phase arrest, then the cells couldn't pass the G2/M checkpoint and enter the mitotic phase, resulting in inhibition of cell proliferation. To further explore the underlying mechanism, we detected a series of cyclins, cyclin-dependent kinases (CDKs), and cyclin-dependent kinase inhibitors (CDKIs), especially P27 and P21. As shown in Fig. 2C–N, the expression levels of cyclin A2, cyclin D3, CDK2, CDK6, Myt1, and P27kip1 were decreased, while the expression levels of cyclin B, cyclin D1, CDK4, p-CDC2, p-wee1, and $P21^{waf1/cip1}$ were increased.

In summary, the upregulation of CDKs inhibitory factor P21 inhibited the expression of CDK2, while the expression of cyclin A2 was significantly downregulated, thereby inhibiting the process of cell transition from S phase to G2 phase. The upregulation of c-Myc expression promoted the expression of CDK4 and activation of CDK4/cyclin D1 complex, thereby promoting the progression of the cell cycle G1 phase to S phase. Meanwhile, the upregulation of p-wee1 promoted the phosphorylation process of CDC2 (CDK1) and inhibited the progression of G2/M phase, which inhibited the transition from the S phase to the G/M phase.

Knockout of PRMT1 promoted cell apoptosis in 16HBE

Previous experiments have confirmed that knocking out PRMT1 could inhibit the proliferation of 16HBE cells. Meanwhile, the oncogene c-Myc, which had both proliferative and apoptotic effects, is upregulated in PRMT1 knocked out cell lines. To determine whether PRMT1 knockout could affect cell apoptosis, we conducted apoptosis analysis via flow cytometry. As shown in Fig. 3A, B, knockout of PRMT1 induced the proportion of apoptotic cells. To further investigate the biological function of PRMT1 deficiency-induced apoptosis in 16HBE cells, we detected the expression levels of anti-apoptotic protein B-cell lymphoma-2 (Bcl-2) and pro-apoptotic protein Bax in the Bcl-2 protein family[35,36]. Western blot showed that the expression of Bax was upregulated, while the expression of Bcl-2 was downregulated (Fig. 3C, D). The results were consistent with the obtained flow cytometry apoptosis analysis results. Therefore, it turned out that knocking out PRMT1 induced apoptosis in 16HBE cells by regulating the expressions of Bcl-2 and Bax.

Knockout of PRMT1 accelerated cell motility in 16HBE

Abnormal proliferation, apoptosis, and migration were key characteristics of tumor metastasis. To investigate the role of PRMT1 in cell migration, we detected the wound-healing capacity of PRMT1 in WT and knockout cell lines. It turned out that in 16P-2 and 16P-11 cell lines, the wound closure after 6 h and 12 h was more promoted than that in the WT cell line (Fig. 4A, B), indicating that knockout of PRMT1 enhanced cell migration. Further cell invasion assay showed that the number of invading cells was statistically higher in PRMT1 knockout 16HBE compared with WT (Fig. 4C, D). During the process of tumor metastasis, there was a phenomenon of tightly connected epithelial cells transforming into loosely connected mesenchymal cells, which is called epithelial-mesenchymal transition (EMT). Calcium-dependent cell–cell adhesion molecule E-cadherin[37], transmembrane glycoprotein N-cadherin[38], and intermediate filament protein vimentin[39] were closely related to the EMT process. Western blot showed that E-cadherin, N-cadherin, and vimentin were downregulated in knockout cell lines (Fig. 4E–G), which indicated that PRMT1 might affect cell motility and be involved in EMT via regulation of E-cadherin, N-cadherin, and vimentin.

Discussion

PRMT1 played an important role in normal physiological processes, including embryogenesis and development. Meanwhile, dysfunction of PRMT1 is associated with a series of lung diseases. However, the potential role of PRMT1 in cell proliferation and migration in bronchial epithelium-related diseases was still unclear. In the current study, 16HBE was chosen to investigate it. First of all, we found that knockout of PRMT1 could inhibit cell proliferation, and the potential explanation should be that knockout of PRMT1 up-regulated the expressions of c-Myc and induced the phosphorylation of AKT, which were two frequently dysregulated proteins in various biological processes, including cell growth, proliferation, and death/survival, thereby inhibited the proliferation of 16HBE cells. The results of cell apoptosis showed that the absence of PRMT1 protein up-regulated proapoptotic protein Bax, while down-regulated anti-apoptotic protein Bcl-2, ultimately inducing apoptosis in 16HBE cells. The cell cycle detection results showed that knockout of PRMT1 decreased the proportion of cells in G1 phase and G2/M phase, while the proportion of S phase cells responsible for DNA synthesis was significantly increased. By detecting the expression of cyclins, CDKs, CDKIs and checkpoints, the potential biological process was following: Firstly, the upregulation of CDKs inhibitory factor P21 (S phase checkpoint) inhibited the expression of CDK2 (S phase checkpoint), while the expression of Cyclin A2 (S phase checkpoint) was significantly downregulated, thereby inhibiting the process of cell transition from the S phase to the G2 phase. Secondly, the upregulation of c-Myc expression promoted the expression of CDK4 (G1/S checkpoint) and the activity of CDK4/cyclin D1 (G1/S checkpoint) complex, thereby promoting the progression of the G1 phase to the S phase of the cell cycle. Thirdly, the upregulation of p-wee1 (G2/M checkpoints) expression promoted the phosphorylation process of CDC2 (G2/M checkpoints), inhibited the progression of G2/M phase, limited the transition of the cell cycle from S phase to G/M phase, and led to the arrest of 16HBE cells in S phase. Further cell migration experiments showed that knocking out the PRMT1 protein could promote wound-healing and speed up cell migration. As shown in Fig. 5, a seemingly paradoxical findings of our study was that PRMT1 knockout simultaneously inhibited cell proliferation and promoted cell migration. Significant downregulation of classical EMT markers, including E-cadherin, N-cadherin and vimentin, was observed, suggesting an absence of mesenchymal transition. However, the enhanced motility indicates a migratory phenotype. We speculate that this uncoupling of proliferation from migration may be driven by the unique signaling environment in PRMT1 knockout cells. The concurrent upregulation of c-Myc and p-AKT, both of which are known to stimulate cell motility, coupled with S-phase arrest, may rewire cellular priorities from growth to movement. In this model,

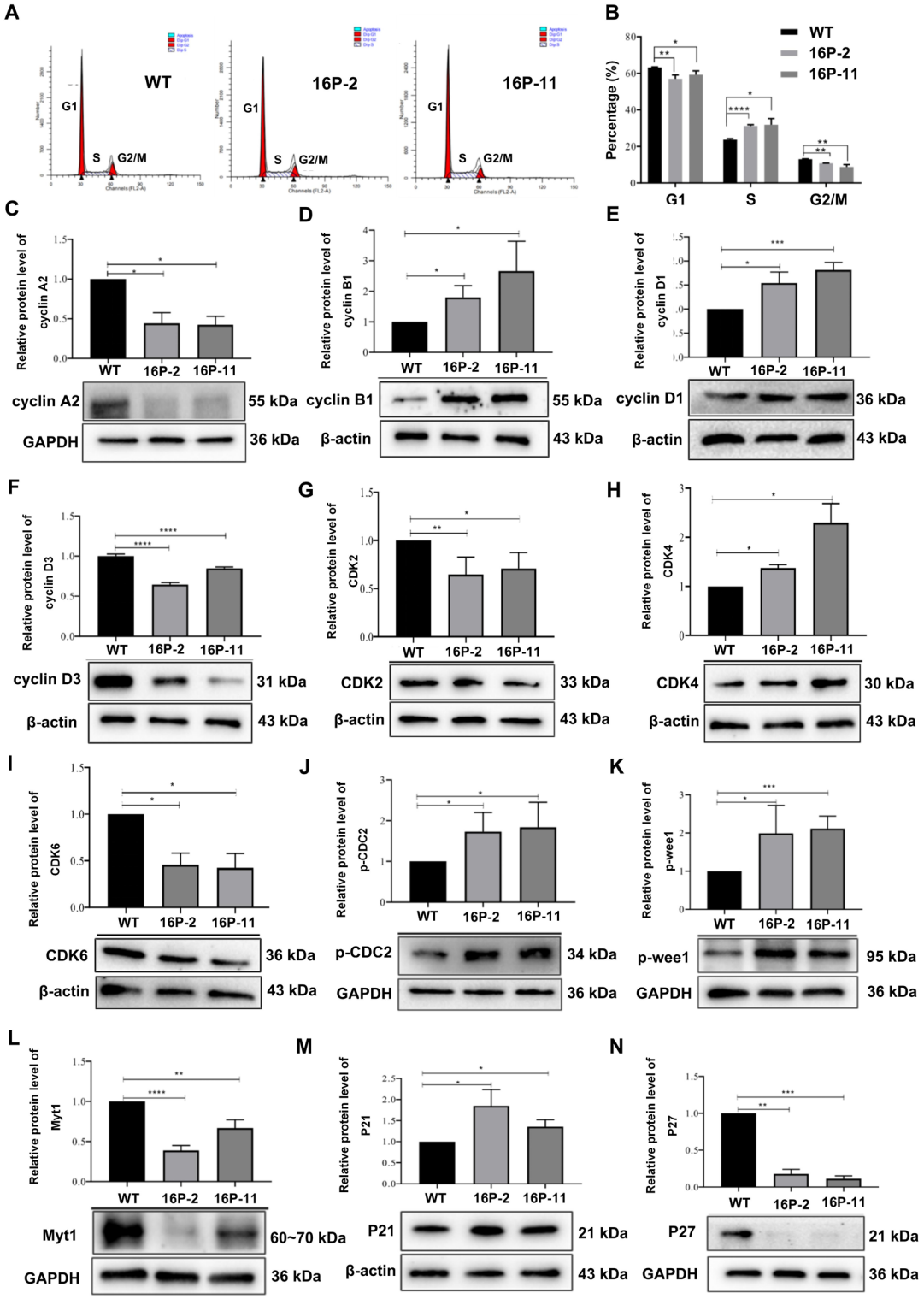

Fig. 2. Knockout of PRMT1 redistributed the cell cycle in 16HBE. (**A**) Knockout of PRMT1 induced cell cycle redistribution. (**B**) The bar graph showed that knockout of PRMT1 reduced the percentage of G1 and G2/M cells, while the percentage of S phase cells was increased. (**C**–**N**) Knockout of PRMT1 altered the expression levels of cyclin A2, cyclin B1, cyclin D1, cyclin D3, CDK2, CDK4, CDK6, p-CDC2, p-wee1, Myt1, P21, and P27, respectively. Upper, bar graph; lower, representative blots. *, $p < 0.05$; **, $p < 0.01$; ***, $p < 0.001$; ****, $p < 0.0001$.

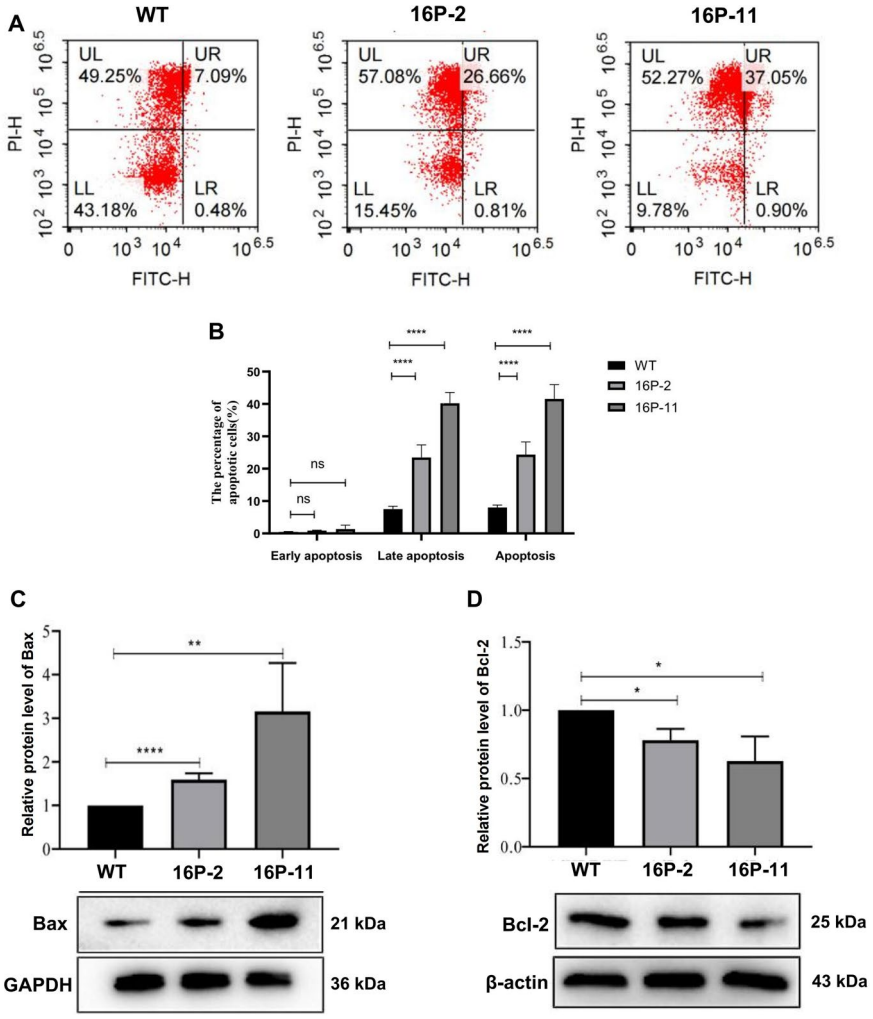

Fig. 3. Knockout of PRMT1 induced cell apoptosis in 16HBE. (**A**) PI-FITC analysis showed apoptotic cells were increased in 16P-2 and 16P-11. The bar graph was presented in (**B**, **C**). The expression of Bax was upregulated in PRMT1 knockout 16HBE. (**D**) Bcl-2 was down-regulated in PRMT1 knockout cell lines. Upper, bar graph; lower, representative blots. ns, not significant; *, $p < 0.05$; **, $p < 0.01$; ****, $p < 0.0001$.

cell cycle arrest halts proliferation while persistent c-Myc and AKT activity, potentially in conjunction with stress signals from the arrested state, provides a potent drive for migration. This phenomenon highlights the context-dependent role of PRMT1, suggesting that its loss can reprogram bronchial epithelial cells into an invasive yet non-proliferative state. This phenotype is particularly relevant for understanding the early stages of disease progression.

Conclusion

In conclusion, our findings suggest that PRMT1 has a dual regulatory role in cell behavior. It is involved in controlling both cell proliferation and migration. The knockout of PRMT1 leads to a complex phenotype where cells are arrested in S phase yet become more migratory. This uncoupling highlights the nuanced role of PRMT1 in cellular function, suggesting that its absence could reprogram proliferative cells into a migratory, invasive state even in the absence of EMT. Further studies are needed to explore the specific signaling pathways that mediate this shift and to determine the broader implications for bronchial epithelial-related lung disorders.

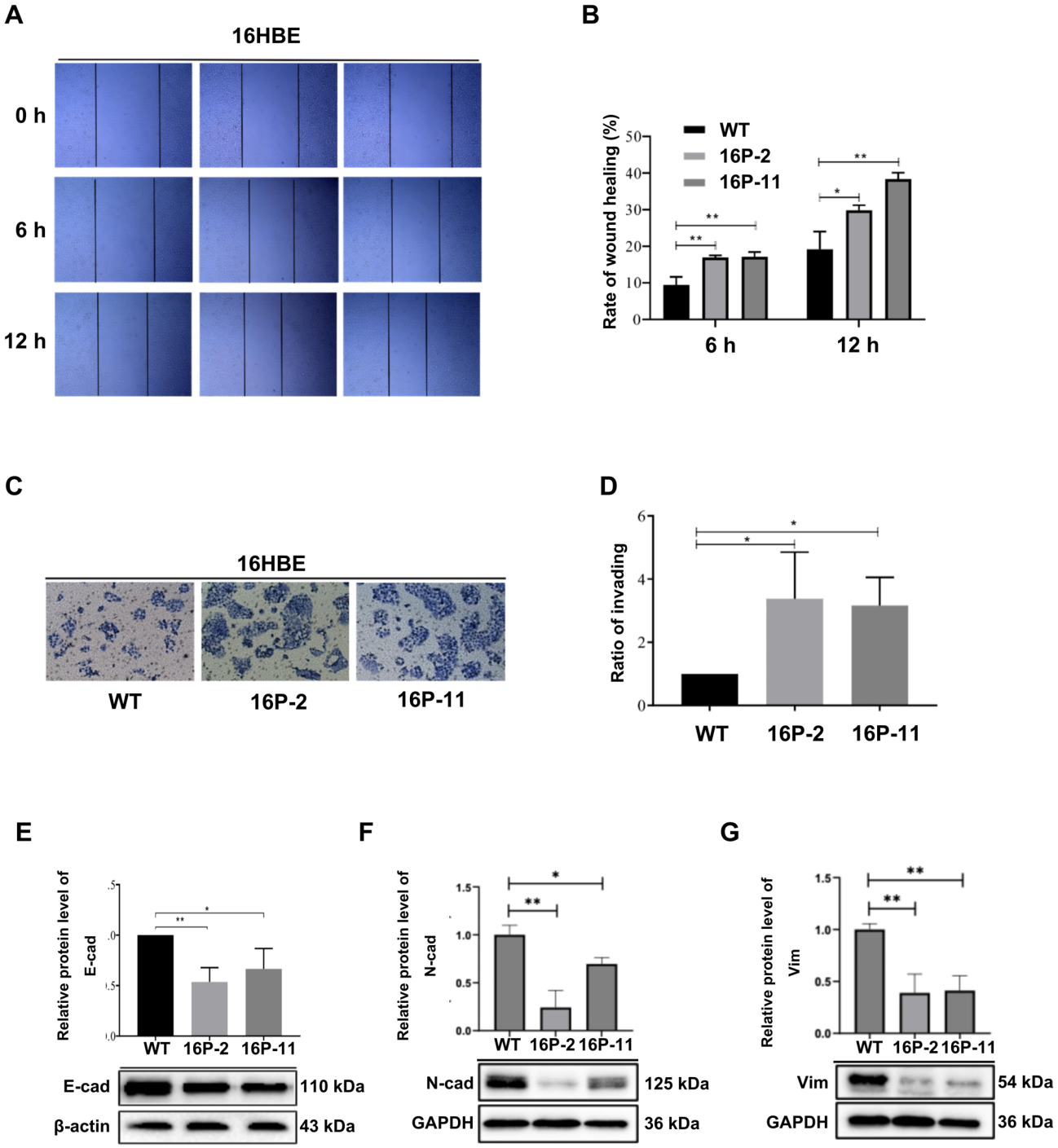

Fig. 4. Knockout of PRMT1 induced cell migration. (**A**) Knockout of PRMT1 accelerated wound healing. (**B**) The bar graph showed the rate of wound healing in WT, 16P-2, and 16P-11. (**C**) Knockout of PRMT1 induced cell invasion. (**D**) The bar graph showed the ratio of invasion in WT, 16P-2, and 16P-11. (**E**) E-cad was decreased in PRMT1 knockout 16HBE. (**F**) N-cad was decreased in PRMT1 knockout 16HBE. (**G**) Vimentin was decreased in PRMT1 knockout 16HBE*, $p < 0.05$; **, $p < 0.01$.

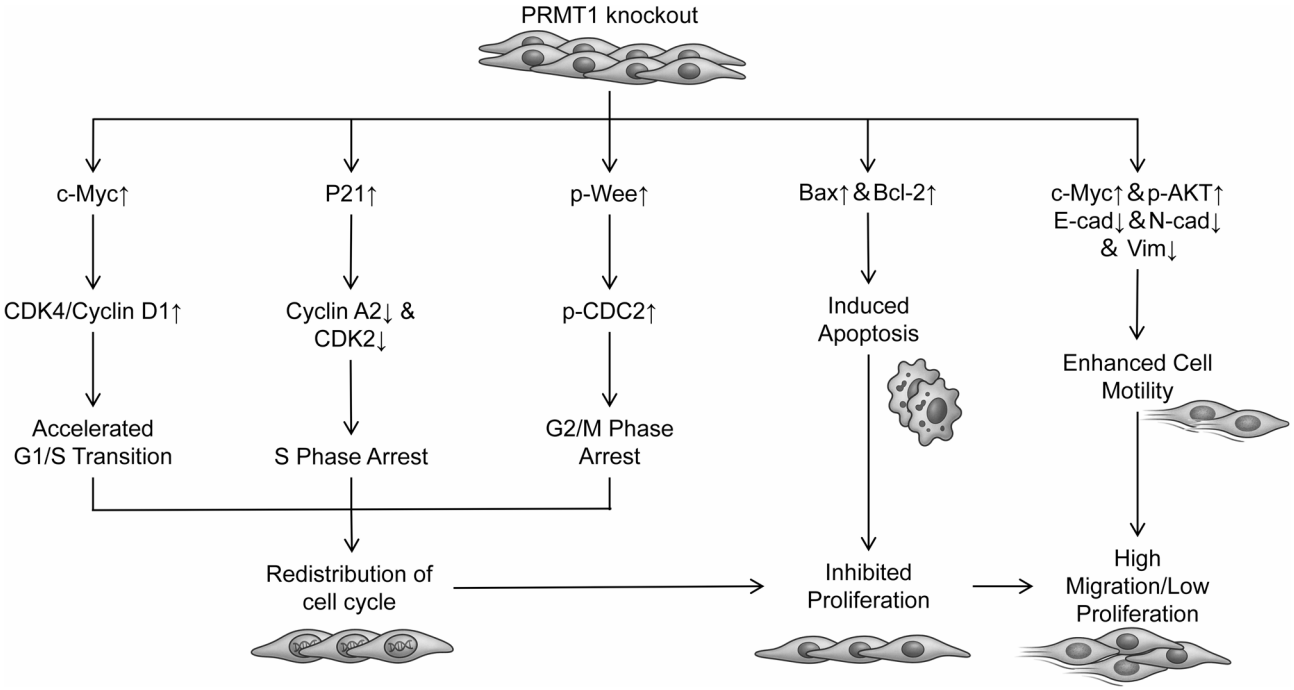

Fig. 5. Schematic model of PRMT1 function in 16HBE.

Data availability

All data generated and analyzed in this study are available upon reasonable request from the corresponding author.

Received: 12 September 2024; Accepted: 31 October 2025
Published online: 03 December 2025

References

1. Wu, Q., Schapira, M., Arrowsmith, C. H. & Barsyte-Lovejoy, D. Protein arginine methylation: From enigmatic functions to therapeutic targeting. *Nat. Rev. Drug Discov.* **20**, 509–530 (2021).
2. Guccione, E. & Richard, S. The regulation, functions and clinical relevance of arginine methylation. *Nat. Rev. Mol. Cell Biol.* **20**, 642–657 (2019).
3. Thiebaut, C., Eve, L., Poulard, C. & Le Romancer, M. Structure, activity, and function of PRMT1. *Life* **11**, 1147 (2021).
4. Shibata, Y., Okada, M., Miller, T. C. & Shi, Y. B. Knocking out histone methyltransferase PRMT1 leads to stalled tadpole development and lethality in *Xenopus tropicalis*. *Biochim. Biophys. Acta Gen. Subj.* **1864**, 129482 (2020).
5. Fujimoto, K., Matsuura, K., Hu-Wang, E., Lu, R. & Shi, Y. B. Thyroid hormone activates protein arginine methyltransferase 1 expression by directly inducing c-Myc transcription during Xenopus intestinal stem cell development. *J. Biol. Chem.* **287**, 10039–10050 (2012).
6. Matsuda, H. & Shi, Y. B. An essential and evolutionarily conserved role of protein arginine methyltransferase 1 for adult intestinal stem cells during postembryonic development. *Stem Cells* **28**, 2073–2083 (2010).
7. Matsuda, H., Paul, B. D., Choi, C. Y., Hasebe, T. & Shi, Y. B. Novel functions of protein arginine methyltransferase 1 in thyroid hormone receptor-mediated transcription and in the regulation of metamorphic rate in Xenopus laevis. *Mol. Cell Biol.* **29**, 745–757 (2009).
8. An, X. et al. Modulation of I(Ks) channel-PIP(2) interaction by PRMT1 plays a critical role in the control of cardiac repolarization. *J. Cell Physiol.* **237**, 3069–3079 (2022).
9. Pyun, J. H. et al. Cardiac specific PRMT1 ablation causes heart failure through CaMKII dysregulation. *Nat. Commun.* **9**, 5107 (2018).
10. Zhao, J., Adams, A., Weinman, S. A. & Tikhanovich, I. Hepatocyte PRMT1 protects from alcohol induced liver injury by modulating oxidative stress responses. *Sci. Rep.* **9**, 9111 (2019).
11. Zhu, Y. et al. Inhibition of PRMT1 alleviates sepsis-induced acute kidney injury in mice by blocking the TGF-beta1 and IL-6 trans-signaling pathways. *FEBS Open Bio* **13**, 1859–1873 (2023).
12. Mayulu, N. et al. Sulfated polysaccharide from *Caulerpa racemosa* attenuates the obesity-induced cardiometabolic syndrome via regulating the PRMT1-DDAH-ADMA with mTOR-SIRT1-AMPK pathways and gut microbiota modulation. *Antioxidants* **12**, 1555 (2023).
13. Wu, T. T. et al. Analyses of PRMT1 proteins in human colon tissues from Hirschsprung disease patients. *Neurogastroenterol. Motil.* **22**, 984-e254 (2010).
14. Xue, L. et al. Protein arginine methyltransferase 1 regulates cell proliferation and differentiation in adult mouse adult intestine. *Cell Biosci.* **11**, 113 (2021).
15. Peng, Z., Bao, L., Shi, B. & Shi, Y. B. Protein arginine methyltransferase 1 is required for the maintenance of adult small intestinal and colonic epithelial cell homeostasis. *Int. J. Biol. Sci.* **20**, 554–568 (2024).
16. Peng, Z. et al. Protein arginine methyltransferase 1 regulates mouse enteroendocrine cell development and homeostasis. *Cell Biosci.* **14**, 70 (2024).

17. Tao, H. et al. PRMT1 inhibition activates the interferon pathway to potentiate antitumor immunity and enhance checkpoint blockade efficacy in melanoma. *Cancer Res.* **84**, 419–433 (2024).
18. Liu, J. et al. PRMT1 mediated methylation of cGAS suppresses anti-tumor immunity. *Nat. Commun.* **14**, 2806 (2023).
19. Nasim, F., Sabath, B. F. & Eapen, G. A. Lung cancer. *Med. Clin. N. Am.* **103**, 463–473 (2019).
20. Mao, Y., Yang, D., He, J. & Krasna, M. J. Epidemiology of lung cancer. *Surg. Oncol. Clin. N. Am.* **25**, 439–445 (2016).
21. Ntontsi, P., Photiades, A., Zervas, E., Xanthou, G. & Samitas, K. Genetics and epigenetics in asthma. *Int. J. Mol. Sci.* **22**, 2412 (2021).
22. Q. Sun et al., Bronchial thermoplasty decreases airway remodelling by blocking epithelium-derived heat shock protein-60 secretion and protein arginine methyltransferase-1 in fibroblasts. *Eur Respir J* **54**, (2019).
23. Sun, Q. et al. Constitutive high expression of protein arginine methyltransferase 1 in asthmatic airway smooth muscle cells is caused by reduced microRNA-19a expression and leads to enhanced remodeling. *J. Allergy Clin. Immunol.* **140**, 510–524 (2017).
24. Zhai, W. et al. PRMT1 modulates processing of asthma-related primary microRNAs (Pri-miRNAs) into mature miRNAs in lung epithelial cells. *J. Immunol.* **206**, 11–22 (2021).
25. Avasarala, S. et al. PRMT1 Is a novel regulator of epithelial-mesenchymal-transition in non-small cell lung cancer. *J. Biol. Chem.* **290**, 13479–13489 (2015).
26. Xu, C. et al. Pterostilbene suppresses oxidative stress and allergic airway inflammation through AMPK/Sirt1 and Nrf2/HO-1 pathways. *Immun. Inflamm. Dis.* **9**, 1406–1417 (2021).
27. Xia, F., Yang, L. & Zhu, X. Knockdown of circ_0038467 alleviates lipopolysaccharides-induced 16HBE cell injury by regulating the miR-545-3p/TRAF1 axis in neonatal pneumonia. *Microb. Pathog.* **173**, 105819 (2022).
28. Zhang, H. et al. Roles of H19/miR-29a-3p/COL1A1 axis in COE-induced lung cancer. *Environ Pollut* **313**, 120194 (2022).
29. Zhou, M. L., Ma, J. N. & Xue, L. Effect of protein arginine methyltransferase 1 gene knockout on the proliferation of human embryonic kidney 293T cells. *Biol. Bull.* **49**, S1–S11 (2023).
30. Wang, H. X. et al. Proteomic analysis reveals that placenta-specific protein 9 inhibits proliferation and stimulates motility of human bronchial epithelial cells. *Front. Oncol.* **11**, 628480 (2021).
31. Griffin, N. I. et al. ADA3 regulates normal and tumor mammary epithelial cell proliferation through c-MYC. *Breast Cancer Res.* **18**, 113 (2016).
32. Dai, L., Wang, W., Liu, Y., Song, K. & Di, W. Inhibition of sphingosine kinase 2 down-regulates ERK/c-Myc pathway and reduces cell proliferation in human epithelial ovarian cancer. *Ann. Transl. Med.* **9**, 645 (2021).
33. Feng, Y. et al. Mechanistic insights into carbon black-activated AKT/TMEM175 cascade impairing macrophage-epithelial cross-talk and airway epithelial proliferation. *Environ. Pollut.* **372**, 126076 (2025).
34. Ciribilli, Y., Singh, P., Spanel, R., Inga, A. & Borlak, J. Decoding c-Myc networks of cell cycle and apoptosis regulated genes in a transgenic mouse model of papillary lung adenocarcinomas. *Oncotarget* **6**, 31569–31592 (2015).
35. Tsujimoto, Y., Ikegaki, N. & Croce, C. M. Characterization of the protein product of bcl-2, the gene involved in human follicular lymphoma. *Oncogene* **2**, 3–7 (1987).
36. Huang, Z. Bcl-2 family proteins as targets for anticancer drug design. *Oncogene* **19**, 6627–6631 (2000).
37. Hazan, R. B., Qiao, R., Keren, R., Badano, I. & Suyama, K. Cadherin switch in tumor progression. *Ann. N Y Acad. Sci.* **1014**, 155–163 (2004).
38. Cao, Z. Q., Wang, Z. & Leng, P. Aberrant N-cadherin expression in cancer. *Biomed. Pharmacother.* **118**, 109320 (2019).
39. Coelho-Rato, L. S., Parvanian, S., Modi, M. K. & Eriksson, J. E. Vimentin at the core of wound healing. *Trends Cell Biol.* **34**, 239–254 (2024).

Acknowledgements

We appreciate all the colleagues who work in Institute for Medical Biology for their scientific and technical support.

Author contributions

LX conceived and designed the experiments. WJY performed the experiments. BYL analyzed the data and generated the figures. LX wrote the manuscript. All authors declared that they have no conflicts of interest in the authorship and publication of this article.

Funding

This project was supported by Fund for Key Laboratory Construction of Hubei Province (Grant No. 2018BFC360), the National Natural Science Foundation of China (Grant No. 31101047 to Lu Xue), "the Fundamental Research Funds for the Central Universities", South-Central MinZu University (Grant Number: CZQ22013), Hubei Medical Biology International Science and Technology Cooperation Base (Grant Number: PTZ24018).

Declarations

Competing interests

The authors declare no competing interests.

Additional information

Supplementary Information The online version contains supplementary material available at https://doi.org/10.1038/s41598-025-26934-w.

Correspondence and requests for materials should be addressed to L.X.